Macroscopic Dynamics of a Trapped Bose-Einstein Condensate in the Presence of 1D and 2D Optical Lattices

M. Krämer,[1] L. Pitaevskii,[1,2] and S. Stringari[1]

[1]*Dipartimento di Fisica, Università di Trento, and Istituto Nazionale per la Fisica della Materia, I-38050 Povo, Italy*

[2]*Kapitza Institute for Physical Problems, ulitza Kosygina 2, 117334 Moscow, Russia*

(Received 22 January 2002; published 22 April 2002)

The hydrodynamic equations of superfluids for a weakly interacting Bose gas are generalized to include the effects of periodic optical potentials produced by stationary laser beams. The new equations are characterized by a renormalized interaction coupling constant and by an effective mass accounting for the inertia of the system along the laser direction. For large laser intensities the effective mass is directly related to the tunneling rate between two consecutive wells. The predictions for the frequencies of the collective modes of a condensate confined by a magnetic harmonic trap are discussed for both 1D and 2D optical lattices and compared with recent experimental data.

DOI: 10.1103/PhysRevLett.88.180404 PACS numbers: 03.75.Fi, 05.30.Jp, 32.80.Pj

The experimental realization of optical lattices [1–6] is stimulating new perspectives in the study of coherence phenomena in trapped Bose-Einstein condensates. A first direct measurement of the critical Josephson current has been recently obtained in [3] by studying the center of mass motion of a magnetically trapped gas in the presence of a 1D periodic optical potential. Under these conditions the propagation of collective modes is a genuine quantum effect produced by the tunneling through the barriers and by the superfluid behavior associated with the coherence of the order parameter between different wells. The effect of the optical potential is to increase the inertia of the gas along the direction of the laser giving rise to a reduction of the frequency of the oscillation.

The purpose of the present work is to investigate the collective oscillations of a magnetically trapped gas in the presence of 1D and 2D optical lattices taking into account the effect of tunneling, the role of the mean field interaction, and the 3D nature of the sample. Under suitable conditions these effects can be described by generalizing the hydrodynamic equations of superfluids [7].

Let us assume that the gas, at $T = 0$, be trapped by an external potential given by the sum of a harmonic trap of magnetic origin $V_{\rm ho}$ and of a stationary optical potential $V_{\rm opt}$ modulated along the z axis. The resulting potential is given by

$$V_{\rm ext} = \tfrac{1}{2}m(\omega_x^2 x^2 + \omega_y^2 y^2 + \omega_z^2 z^2) + sE_R \sin^2 qz\,, \tag{1}$$

where ω_x, ω_y, ω_z are the frequencies of the harmonic trap, $q = 2\pi/\lambda$ is fixed by the wavelength of the laser light creating the stationary 1D lattice wave, $E_R = \hbar^2 q^2/2m$ is the so-called recoil energy, and s is a dimensionless parameter providing the intensity of the laser beam. The optical potential has periodicity $d = \pi/q = \lambda/2$ along the z axis. The case of a 2D lattice will be discussed later. In the following we will assume that the laser intensity is large enough to create many separated wells giving rise to an array of several condensates. Still, because of quantum tunneling, the overlap between the wave functions of two consecutive wells can be sufficient to ensure full coherence. In this case one is allowed to use the Gross-Pitaevskii (GP) theory for the order parameter to study both the equilibrium and the dynamic behavior of the system at zero temperature [8]. Eventually, if the tunneling becomes too small, the fluctuations of the relative phase between the condensates will destroy the coherence of the sample giving rise to new quantum configurations associated with the transition to a Mott insulator phase [2,6].

In the presence of coherence it is natural to make the ansatz

$$\Psi(\mathbf{r}) = \sum_k \Psi_k(x,y) f_k(z) e^{iS_k(x,y)} \tag{2}$$

for the order parameter in terms of a sum of many condensate wave functions relative to each well. Here $S_k(x,y)$ is the phase of the k component of the order parameter, while Ψ_k and f_k are real functions. We will make the further periodicity assumption $f_k(z) = f_0(z - kd)$ where f_0 is localized at the origin. The above assumptions for Ψ and f_k are justified for relatively large values of s where the interwell barriers are significantly higher than the chemical potential. In this case the condensate wave functions of different sites are well separated (tight binding approximation).

Using the ansatz (2) for the order parameter one finds the following result for the mean field expectation value of the effective Hamiltonian $H = \sum_j [\mathbf{p}_j^2/2m + V_{\rm ext}(\mathbf{r}_j)] + g\sum_{j<k}\delta(\mathbf{r}_j - \mathbf{r}_k)$:

$$E = \langle H \rangle = \left[\int dz \, \frac{\hbar^2}{2m} (\partial_z f_0)^2 + f_0^2 V_{\rm opt} \right] \sum_k \int dx\, dy\, \Psi_k^2 + \frac{g}{2} \left[\int dz\, f_0^4 \right] \sum_k \int dx\, dy\, \Psi_k^4 + \left[\int dz\, f_0^2 \right] \sum_k \int dx\, dy \left[\frac{\hbar^2}{2m} (\partial_{\mathbf{r}_\perp} \Psi_k)^2 + \Psi_k^2 V_{\rm ho}(\mathbf{r}_\perp, kd) + \frac{\hbar^2}{2m} \Psi_k^2 (\partial_{\mathbf{r}_\perp} S_k)^2 \right] - \delta \sum_k \int dx\, dy\, \Psi_k \Psi_{k+1} \cos[S_k - S_{k+1}], \quad (3)$$

where in the two-body and in the magnetic interaction terms as well as in the radial kinetic energy we have ignored the overlap contributions arising from different wells. In the evaluation of the axial kinetic energy and of the optical potential term we have instead kept also the overlap terms originating from consecutive wells. These are proportional to the quantity

$$\delta = -2 \int dz \left[\frac{\hbar^2}{2m} \partial_z f_0(z) \partial_z f_0(z - d) + f_0(z) f_0(z - d) V_{\rm opt} \right], \quad (4)$$

related to the tunneling rate and responsible for the occurrence of Josephson effects.

By setting $S_k = 0$ (ground-state configuration), the variation of E with respect to f_0 yields the equation

$$\left[-\frac{\hbar^2}{2m} \frac{\partial^2}{\partial z^2} + s E_R \sin^2 qz \right] f_0(z) = \varepsilon_0 f_0(z), \quad (5)$$

where ε_0 is introduced to ensure the normalization condition $\int_{-d/2}^{d/2} dz\, f_0^2 = 1$ which implies that the functions Ψ_k are normalized to the number of atoms N_k occupying each site: $\int \Psi_k^2\, dx\, dy = N_k$. In Eq. (5) we have ignored the contribution arising from the two-body interaction. Estimates of [9] show that this is a good approximation already at moderately large s. Since in the following we are interested in the low energy excitations, we will keep the function f_0 equal to the ground-state solution of (5).

In order to discuss the macroscopic properties of the system, including its low energy dynamics, it is convenient to transform the discretized formalism described above into the one of continuum variables. This is obtained through the replacement $\sum_k \to (1/d) \int dz$ in the various terms of the energy. Through such a procedure one naturally introduces a smoothed or "macroscopic" density defined by

$$n_M(x, y, z) = (1/d) \Psi_k^2(x, y) \quad (6)$$

with $z \simeq dk$, and a smoothed phase S [$S_k \to S(x, y, z)$].

By applying the smoothing procedure to Eq. (3) we obtain the following macroscopic expression for the energy functional

$$E = \int dV\, n_M \left[\frac{\tilde{g} n_M}{2} + V_{\rm ho} + \frac{\hbar^2}{2m} (\partial_{\mathbf{r}_\perp} S)^2 - \delta \cos[d \partial_z S] \right], \quad (7)$$

where we have introduced the renormalized coupling constant $\tilde{g} = g d \int f_0^4\, dz$, we have neglected quantum pressure terms originating from the radial term in the kinetic energy, and we have set $\Psi_k \Psi_{k+1} \sim \Psi_k^2 = d n_M$. We have also omitted some constant terms [first two terms in Eq. (3)] which do not depend on n_M or on S.

With respect to the functional characterizing a trapped Bose gas in the absence of optical confinement, one notices two important differences: first, the interaction coupling constant is renormalized due to the presence of the optical lattice. This is the result of the local compression of the gas produced by the tight optical confinement which increases the repulsive effect of the interactions. Second, the kinetic energy term along the z direction has no longer the classical quadratic form as in the radial direction, but exhibits a periodic dependence on the gradient of the phase. By expanding this term for small gradients, which is the case in the study of small amplitude oscillations, one derives a quadratic term of the form $(\hbar^2/2m^*) \int dV\, n_M (\partial_z S)^2$ characterized by the effective mass

$$\frac{m}{m^*} = \frac{m \delta d^2}{\hbar^2} = \frac{\delta}{E_R} \frac{\pi^2}{2}, \quad (8)$$

where δ is defined by Eq. (4). Notice that within the employed approximation the value of δ, and hence of m^*, does not depend on the number of atoms, nor on the mean field interaction.

The equilibrium density profile, obtained by minimizing Eq. (7) with $S = 0$ has the typical form of an inverted parabola [10]

$$n_M^0 = [\mu - \tfrac{1}{2} m (\omega_x^2 x^2 + \omega_y^2 y^2 + \omega_z z^2)]/\tilde{g}, \quad (9)$$

which conserves the aspect ratio of the original magnetic trapping. The size of the condensate has instead increased since $\tilde{g} > g$. For large s the increase of the coupling constant can be large ($\tilde{g} \sim s^{1/4}$ [9]). However, since the radius of the sample scales like the $\frac{1}{5}$th power of $\tilde{g}$, the resulting increase in the size of the system is not very spectacular (for $s = 15$ we find an increase of the size by $\sim$20% for the experimental setting of [3]).

The functional (7) can be used to carry out dynamic calculations. In this case one needs the action $A = \int dt\, (\langle H \rangle - i\hbar \langle \frac{\partial}{\partial t} \rangle)$, with the second term given by $i\hbar \langle (\partial/\partial t) \rangle = -\int dV\, \hbar n_M \dot{S}$. The resulting equations of motion are obtained by imposing the stationarity condition on the action with respect to arbitrary variations of the density n_M and of the phase S

$$\dot{n}_M + \frac{\hbar}{m}\,\partial_{\mathbf{r}_\perp}(n_M \partial_{\mathbf{r}_\perp} S) + \frac{\delta d}{\hbar}\,\partial_z(n_M \sin[d\,\partial_z S]) = 0\,, \tag{10}$$

$$\hbar\dot{S} + \tilde{g} n_M + V_{\rm ho} + \frac{\hbar^2}{2m}(\partial_{\mathbf{r}_\perp} S)^2 - \delta\cos[d\,\partial_z S] = 0\,. \tag{11}$$

In particular, at equilibrium these equations reproduce result (9) for the equilibrium density. Furthermore, Josephson-type oscillations are among those captured by Eqs. (10) and (11). To see this, consider the case of a uniform gradient of the phase along z, $\partial_z S = P_Z(t)/\hbar$, where P_Z is a time-dependent parameter. From Eqs. (10) and (11) one can then derive equations of motion for the center of mass $Z(t) = \int dV\, z n_m(t)/N$ and for the conjugate momentum variable P_Z [3,11]

$$\hbar\dot{Z} - \delta d \sin\left[d\,\frac{P_Z}{\hbar}\right] = 0\,, \tag{12}$$

$$\dot{P}_Z + m\omega_z^2 Z = 0\,, \tag{13}$$

which have the typical Josephson form.

In the limit of small oscillations the solutions of Eqs. (10) and (11) have the form $n = n_M^0 + \delta n(\mathbf{r}) e^{i\omega t}$ with δn obeying the hydrodynamic equations:

$$-\omega^2 \delta n = \partial_{\mathbf{r}_\perp}\left[\frac{\mu - V_{\rm ho}}{m}\,\partial_{\mathbf{r}_\perp}\delta n\right] + \partial_z\left[\frac{\mu - V_{\rm ho}}{m^*}\,\partial_z \delta n\right], \tag{14}$$

where $\mu = \tilde{g} n_M^0(0)$ is the chemical potential of the sample and $n_M^0(0)$ is the equilibrium density (9) evaluated at the center. Equations (14) are applicable to systems whose size is large compared to the oscillator lengths of the magnetic trap (Thomas-Fermi approximation) and for the low energy excitations with $\hbar\omega \ll \mu$. In the absence of magnetic trapping one finds phonons propagating at the velocity $c = \sqrt{\tilde{g} n_M^0/m^*}$, in agreement with the result obtained in [12] for a 1D array of Josephson junctions. In the presence of harmonic trapping the discretized frequencies of the time-dependent solutions of (14) do not depend on the value of the coupling constant. By applying the transformation $z \to \sqrt{m^*/m}\, z$, one actually finds that the new frequencies are simply obtained from the results of [7] by replacing

$$\omega_z \to \omega_z \sqrt{m/m^*}\,. \tag{15}$$

For an elongated trap ($\omega_x = \omega_y = \omega_\perp \gg \omega_z$) the lowest solutions are given by the center-of-mass motion $\omega_D = \sqrt{m/m^*}\,\omega_z$ and by the quadrupole mode $\omega_Q = \sqrt{5/2} \times \sqrt{m/m^*}\,\omega_z$. The center-of-mass frequency coincides with the value obtained from Eqs. (12) and (13) in the limit of small oscillations, in agreement with the result of [3] obtained in the tight binding limit starting from the 1D discrete nonlinear Schrödinger equation. Concerning the quadrupole frequency, we note that the occurrence of the factor $\sqrt{5/2}$ is a nontrivial consequence of the mean field interaction predicted by the hydrodynamic theory of superfluids in the presence of harmonic trapping [7]. In addition to the low-lying axial motion, the system exhibits radial oscillations at high frequency, of the order of $\omega_\perp$. The most important ones are the transverse breathing and quadrupole oscillations occurring at $\omega = 2\omega_\perp$ and $\omega = \sqrt{2}\,\omega_\perp$, respectively. For elongated traps the frequencies of these modes should not be affected by the optical potential. Different scenarios are obtained for disk-shaped traps ($\omega_z \gg \omega_\perp$). The above results apply to the linear regime of small oscillations. Equations (12) and (13) show that in the case of center-of-mass oscillations, the linearity condition is achieved for initial displacements Δx of the trap satisfying $\Delta x \ll \sqrt{2\delta/m\omega_z^2}$, a condition that becomes more and more severe as the laser intensity increases. For larger initial displacements the oscillation is described by the pendulum equations. For very large amplitudes the motion is, however, dynamically unstable [11].

From the previous discussion it emerges that the effective mass is the crucial parameter needed to predict the value of the small amplitude collective frequencies. An estimate of m/m^* can be made by neglecting the magnetic trapping as well as the role of the mean field interaction. Within this approximation the effective mass is easily obtained from the excitation spectrum of the Schrödinger equation for the 1D Hamiltonian $H = -(\hbar^2/2m)\partial^2/\partial z^2 + sE_R \sin^2 qz$, avoiding the explicit determination of the tunneling parameter (4). One looks for solutions of the form $e^{ipz/\hbar} f_p(z)$ where p is the quasimomentum of the atom and $f_p(z)$ is a periodic function of period d. The resulting dispersion law $\varepsilon(p)$ provides, for small p, the effective mass according to the identification $\varepsilon(p) \simeq \varepsilon_0 + p^2/2m^*$. The value of m/m^*, which turns out to be a universal function of the intensity parameter s, has been evaluated for a wide range of values of s (see Fig. 1). These results for m^* can be used to estimate the actual value of the collective frequencies. The method described here to calculate m^* is expected to be reliable not only for very large laser intensities s when the tight binding

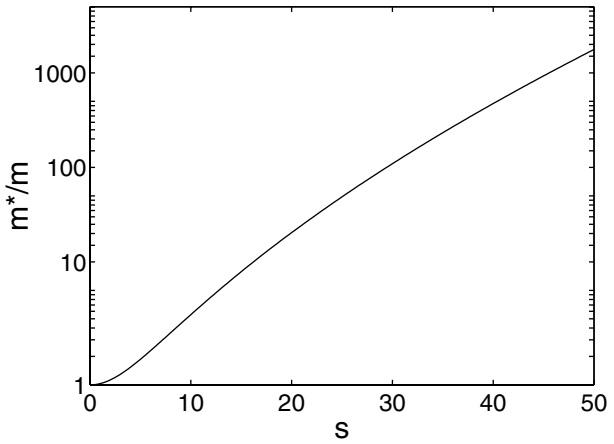

FIG. 1. Effective mass as a function of the laser intensity s [see Eq. (1)] calculated neglecting the effects of interaction and harmonic trapping.

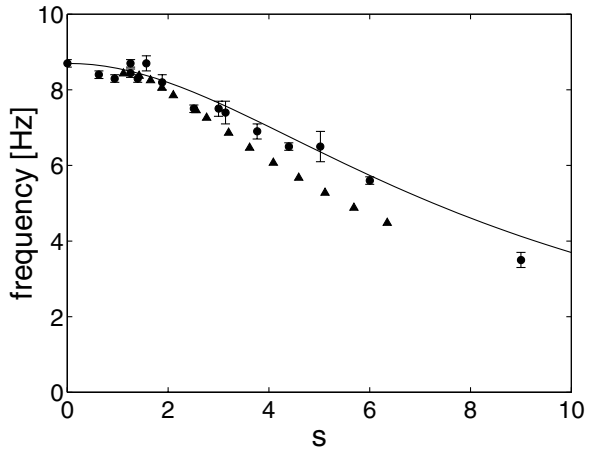

FIG. 2. Frequency of the center-of-mass motion for a condensate trapped by the combined magnetic and optical potential (1) as a function of the laser intensity. The circles and triangles are, respectively, the experimental and theoretical data of [3]. The triangles have been obtained by evaluating the tunneling rate (4) within a Gaussian approximation for the order parameter in each well [3]. The solid line refers to our theoretical prediction (15).

approximation applies and the effective mass can be expressed in terms of the tunneling rate [see Eqs. (8) and (4)], but also for smaller values of s. Of course, for very small laser intensities, as in the experiment [13], the determination of m^* requires the inclusion of the mean field interaction and of the magnetic trapping through the explicit solution of the GP equation.

In Fig. 2 we compare our predictions for the frequencies of the center-of-mass motion with the recent experimental data obtained in [3]. The comparison reveals good agreement with the experiments. Our results also agree well with those obtained from the numerical solution of the time-dependent GP equation [11].

The above formalism is naturally generalized to include a 2D optical lattice where the optical potential is $V_{\rm opt} = sE_R \sin^2 qx + sE_R \sin^2 qy$. The actual potential now generates an array of 1D condensates which has already been the object of experimental studies [4]. For a 2D lattice the ansatz for the order parameter is [14]

$$\Phi(\mathbf{r}) = \sum_{k_x,k_y} \Psi_{k_x,k_y}(z) f_{k_x,k_y}(x,y) e^{iS_{k_x,k_y}(z)}. \qquad (16)$$

In the Thomas-Fermi limit the ground-state smoothed density $n_M = \Psi^2_{k_x,k_y}/d^2$ still has the familiar form $n_M^0 = (\mu - V_{\rm ho})/\tilde{g}$ with the redefined coupling constant $\tilde{g} = g(d\int dx\, f_0^4)^2$, where f_0 is still given by the solution of Eq. (5) and we have used the same approximations as in the 1D case.

Also with regard to dynamics, one can proceed as for the 1D lattice. One finds that the equations of motions, after linearization, take the form

$$\ddot{\delta n} = \partial_z\left[\frac{\mu - V_{\rm ho}}{m}\,\partial_z \delta n\right] + \partial_{\mathbf{r}_\perp}\left[\frac{\mu - V_{\rm ho}}{m^*}\,\partial_{\mathbf{r}_\perp}\delta n\right]. \qquad (17)$$

The frequencies of the low energy collective modes are then obtained from those in the absence of the lattice [7] by simply replacing $\omega_x \to \sqrt{m/m^*}\,\omega_x$ and $\omega_y \to \sqrt{m/m^*}\,\omega_y$. For large laser intensities the value of m^* coincides with the one calculated for the 1D array. If $\omega_z \gg \omega_x\sqrt{m/m^*}, \omega_y\sqrt{m/m^*}$, the lowest energy solutions involve the motion in the x-y plane. The oscillations in the z direction are instead fixed by the value of ω_z. These include the center-of-mass motion ($\omega = \omega_z$) and the lowest compression mode ($\omega = \sqrt{3}\,\omega_z$) [7,8]. The frequency $\omega = \sqrt{3}\,\omega_z$ coincides with the value obtained by directly applying the hydrodynamic theory to 1D systems [15,16] and reveals the 1D nature of the tubes generated by the 2D lattice. If the radial trapping generated by the lattice becomes too strong, the motion along the tubes can no longer be described by the mean field equations and one jumps into more correlated 1D regimes [17].

Stimulating discussions with F. Cataliotti, C. Fort, M. Inguscio, A. Smerzi, and A. Trombettoni are acknowledged. This research is supported by the Ministero della Ricerca Scientifica e Tecnologica (MURST).

[1] B. P. Anderson and M. A. Kasevich, Science **282**, 1686 (1998).
[2] C. Orzel, A. K. Tuchman, M. L. Fensclau, M. Yasuda, and M. A. Kasevich, Science **291**, 2386 (2001).
[3] F. S. Cataliotti, S. Burger, C. Fort, P. Maddaloni, F. Minardi, A. Trombettoni, A. Smerzi, and M. Inguscio, Science **293**, 843 (2001).
[4] M. Greiner, I. Bloch, O. Mandel, T. W. Hänsch, and T. Esslinger, Phys. Rev. Lett. **87**, 160405 (2001).
[5] O. Morsch, J. H. Müller, M. Cristiani, D. Ciampini, and E. Arimondo, Phys. Rev. Lett. **87**, 140402 (2001).
[6] M. Greiner, O. Mandel, T. Esslinger, T. W. Hänsch, and I. Bloch, Nature (London) **415**, 39 (2002).
[7] S. Stringari, Phys. Rev. Lett. **77**, 2360 (1996).
[8] F. Dalfovo, S. Giorgini, L. P. Pitaevskii, and S. Stringari, Rev. Mod. Phys. **71**, 463 (1999).
[9] P. Pedri, L. Pitaevskii, S. Stringari, C. Fort, S. Burger, F. S. Cataliotti, P. Maddaloni, F. Minardi, and M. Inguscio, Phys. Rev. Lett. **87**, 220401 (2001).
[10] The profile (9) can also be obtained by applying the smoothing procedure (6) to the equilibrium solution for Ψ_k^2 given by Eq. (8) in [9].
[11] A. Trombettoni, Ph.D. thesis, SISSA, Trieste, 2001; A. Trombettoni and A. Smerzi (unpublished).
[12] J. Javanainen, Phys. Rev. A **60**, 4902 (1999).
[13] S. Burger, F. S. Cataliotti, C. Fort, F. Minardi, M. Inguscio, M. L. Chiofalo, and M. P. Tosi, Phys. Rev. Lett. **86**, 4447 (2001).
[14] In analogy with the results of [9] we find that, at equilibrium, $\Psi^2_{k_x,k_y}$ is given by an inverted parabola as a function of z. The number of particles $N_{k_x,k_y} = \int dz\, \Psi^2_{k_x,k_y}$ occupying the corresponding site is given by $N_{k_x,k_y} = N_{0,0}(1 - k_x^2/K_x^2 - k_x^2/K_y^2)^{3/2}$ with $K_{x,y} = \sqrt{\hbar\bar{\omega}/m\omega^2_{x,y}d^2} \times [15Na(d\int dx\, f_0^4)^2/a_{\rm ho}]^{1/5}$ and $N_{0,0} = \frac{5}{2\pi}N/K_xK_y$.
[15] S. Stringari, Phys. Rev. A **58**, 2385 (1998).
[16] T.-L. Ho and M. Ma, J. Low Temp. Phys. **115**, 61 (1999).
[17] C. Menotti and S. Stringari, cond-mat/0201158.